

Application of Bucky Gel in Fabrication of a Low-Voltage Rapid Microvalve for Flow Regulation

Ali K. Ghamsari,^{*,†,‡} Ephraim Zegeye,^{†,‡} Yoonyoung Jin,[†] and Eyassu Woldesenbet^{†,‡}

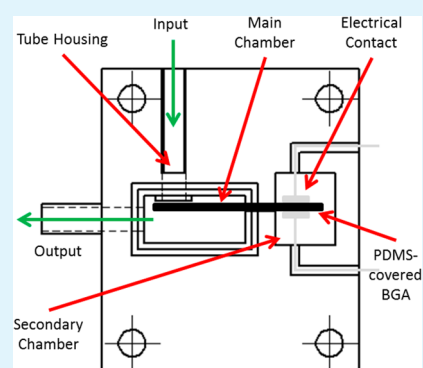
[†]Next Generation Composite CREST Center (NextGenC³), Department of Mechanical Engineering, Southern University and A & M College, Baton Rouge, Louisiana 70813, United States

[‡]Department of Mechanical Engineering, Louisiana State University, Baton Rouge, Louisiana 70803, United States

S Supporting Information

ABSTRACT: Bucky gel is a gelatinous mixture of carbon nanotubes and an ionic liquid. This mixture was employed in fabrication of a low-voltage, rapid, and dry electroactive bimorph actuator: Bucky Gel Actuator (BGA). Feasibility studies were carried out on BGA to evaluate its potential application as a new interface for flow regulation in microfluidics. Following the promising results, a flow regulator was designed and fabricated utilizing BGA as a microvalve. Flow rate measurements showed the capability of BGA microvalve in controlling the output flow rate in the range of 0.1–1 mL/min. BGA microvalve demonstrated great potential to be used for flow regulation in microfluidic devices for point-of-care devices and biomedical applications.

KEYWORDS: bucky gel, electroactive polymers, microvalve, microactuator, flow regulation



1. INTRODUCTION

“Bucky gel” is a room temperature gelatinous mixture of an ionic liquid and carbon nanotubes (CNTs).¹ Outstanding mechanical and electrical properties of CNT, coupled with the high conductivity and stability of ionic liquids made this mixture an attractive alternative in the field of smart materials. Bucky gel has the potential to be applied in sensors, actuators, solar cells, super capacitors, biodetection, and nanocomposites.² Application of CNT and ionic liquid combination in several electrochemical devices for reduction of oxygen³ and sensing^{2,4–9} has already been reported.

“Bucky gel actuator” (BGA) has been one of the most successful applications of bucky gel. BGA is a trilayered bimorph nanocomposite system consisting of an electrolyte layer sandwiched between two electrode layers (Figure 1). The electrode layers are composed of bucky gel embedded in a polymer matrix, whereas the electrolyte layer is a mixture of the ionic liquid and the same polymer matrix.¹ BGA bends toward one side, when a voltage is applied to the electrodes. The direction of bending changes with polarity.

BGA has characteristics that make it an excellent candidate for different actuating applications. Utilizing a solid electrolyte layer, BGA is classified as a “dry” actuator, which unlike many similar alternatives does not require an electrolyte solution to operate. BGA is also driven with just a few volts at a wide range of frequency. Compared to other electroactive materials, BGA has a rapid response, improved lifetime, and a simple fabrication procedure.

To date, most research conducted on BGA has been focused on characterization^{10–12} and performance enhancement,^{13–17} rather than its applications. Mechanical characterization of BGA via nanoindentation and dynamical mechanical analysis has been reported by the authors.¹⁰ BGA maximum lateral displacement, shelf life (change in displacement after being stored), and lifetime (change in displacement over time) has also been studied by our group to identify the effect of applied voltage and frequency, CNT type, thickness, and weight fraction of constituents.¹¹ On the basis of the later study, a displacement model was also developed for BGA samples made of different CNT and ionic liquid types. Different approaches have also been adopted to improve BGA performance. BGA performance enhancement via chemical modification of CNT,^{13–15} conductive and nonconductive additives,¹⁸ and utilization of different nanofillers such as carbon nanofibers,¹⁹ activated carbon nanofibers,¹⁹ Au paste,¹² and nanoporous carbide driven carbon²⁰ has also been investigated. Although there has been significant improvements over time, practical application of BGA is still facing some challenges, such as generated actuation force, the trade-off between stiffness and displacement, etc. However, despite these challenges, BGA has been successfully applied in fabrication of a flexible braille display.^{21,22} Here, we are also reporting the first application of

Received: September 20, 2012

Accepted: May 22, 2013

Published: May 22, 2013

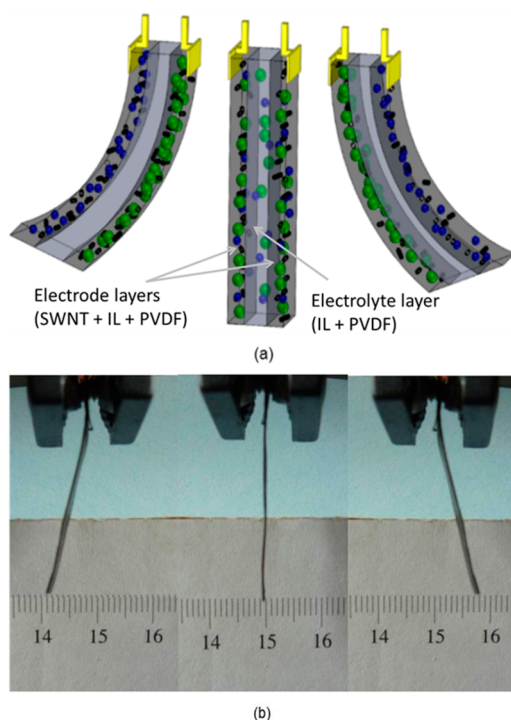


Figure 1. (a) BGA bending motion as a result of ion transfer between layers, direction of bending can be reversed by change in polarity; (b) BGA strip bended (10 V, 0.1 Hz).¹¹

BGA in microfluidics as an active microvalve for flow regulation.

Microfluidics is a promising field of application for BGA. Different electroactive materials and approaches have been used in microfluidics; such as conducting polymers,²³ hydrogel,²⁴ ionic polymer metal composite (IPMC),²⁵ electromagnetic,^{26,27} dielectric elastomer actuators (DEAs),²⁸ and shape memory alloys (SMA).²⁹ These types of materials are typically utilized for the purpose of micropumping, -valving, or -mixing. However, applications using each of these alternatives suffer from varying drawbacks. Hydrogel application in microfluidics, for example, is limited by bubble generation (hydrolysis), slow response time, and lack of precise motion control.²⁴ Utilizing IPMC is also limited by a complicated fabrication process and degradation in performance over time.²⁵ Conducting polymers show slow response and short lifetime, because the bending motion is the result of a reduction oxidation (Redox) process.²³ Electromagnetic and SMA applications are also challenged by complicated structure and slow response time, respectively. Despite their recent improvements in performance and manufacturability, DEA application is still challenging, because

the driving voltage is still more than 1 kV.²⁸ Most of these issues would be avoided by utilizing BGA. BGA has low driving voltage, low power consumption, simple fabrication, long shelf life, and improved lifetime. In addition, BGA design and operation is very flexible. The generated force/displacement of BGA can be controlled through driving conditions (voltage, frequency, signal shape) as well as material and geometrical parameters (type of CNT and ionic liquid, number and thickness of layers, etc.). Despite all these advantages, there were two preliminary concerns about utilizing BGA in microfluidics: actuation force and bubble generation (hydrolysis).

A feasibility study was carried out to evaluate the capability of BGA in generating enough actuation force for flow control. Operation of BGA underwater at different voltages was also monitored to check for potential bubble generation. Following the promising results of the feasibility study, a flow regulator utilizing BGA as a microvalve was designed and fabricated. BGA microvalve was then operated at different voltages and frequencies, and the output flow rate was measured to evaluate BGA microvalve efficiency.

2. EXPERIMENTAL SECTION

2.1. BGA Fabrication. All BGA samples in this study were fabricated using pristine Single-Walled CNTs (Cheap Tubes Inc., USA). Also, EMIMBF₄ (1-ethyl-3-methylimidazolium tetrafluoroborate), PVDF (polyvinylidene fluoride) and DMAC (dimethylacetamide) were selected as the ionic liquid, polymer matrix, and the solvent, respectively. BGA electrode layer contained 22 wt % CNT, 45 wt % ionic liquid and 33 wt % PVDF. The fabrication procedure for the electrode layers began with mixing 0.2 g SWNT, 0.4 g IL, and 4 mL DMAC with a ball-mill for the duration of 30 min. The outcome was a gelatinous black mixture to which 0.32 g PVDF and 8 mL DMAC were added. This mixture was ball-milled again for another 30 min, sonicated for 24 h, casted in silicon rubber molds and cured in an oven for 12 h at 50 °C. Finally, samples were put in a vacuum oven at reduced pressure for another 100 h in order to let DMAC evaporate completely. For the fabrication of electrolyte layers, we mixed IL and PVDF together (1:1 ratio), dissolved them in DMAC, and then casted them similar to the electrode layers.

Fabricated individual layers were then hot pressed together to produce BGA strips. A layer of PDMS was put onto the BGA microvalve to increase the adhesion between the microvalve and fluid inlet for better sealing. This PDMS layer would also prevent the ionic liquid to escape into the aqueous flow, since EMIMBF₄ is soluble in water. The PDMS layer was casted on BGA utilizing SYLGARD 184 Silicone Elastomer kit. The PDMS base and curing agent were mixed (ratio of 10:1) and

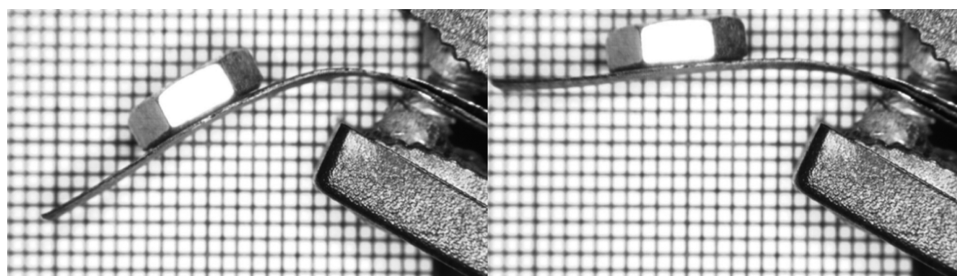


Figure 2. BGA capability in lifting weights in the order of the couple grams (besides its own weight).

manually casted on the BGA strips. The BGA samples were then put in the oven at 100 °C for 40 min to complete the curing process. The final thickness of PDMS layer was between 20 and 40 μm .

2.2. Feasibility Study. Force Measurement. BGA generated force was studied in order to address the actuation force issue. As shown in Figure 2, BGA generated force was obtained based on the height it could lift a fixed weight at different applied voltages. The amount of force was calculated based on the beam deflection and bending moment relation. It was observed that force generated by BGA is a function of its thickness, thickness ratio (thickness of electrolyte layer to the total thickness of electrode layers), and the applied voltage (Figure 3). On the basis of our previous study, thickness and

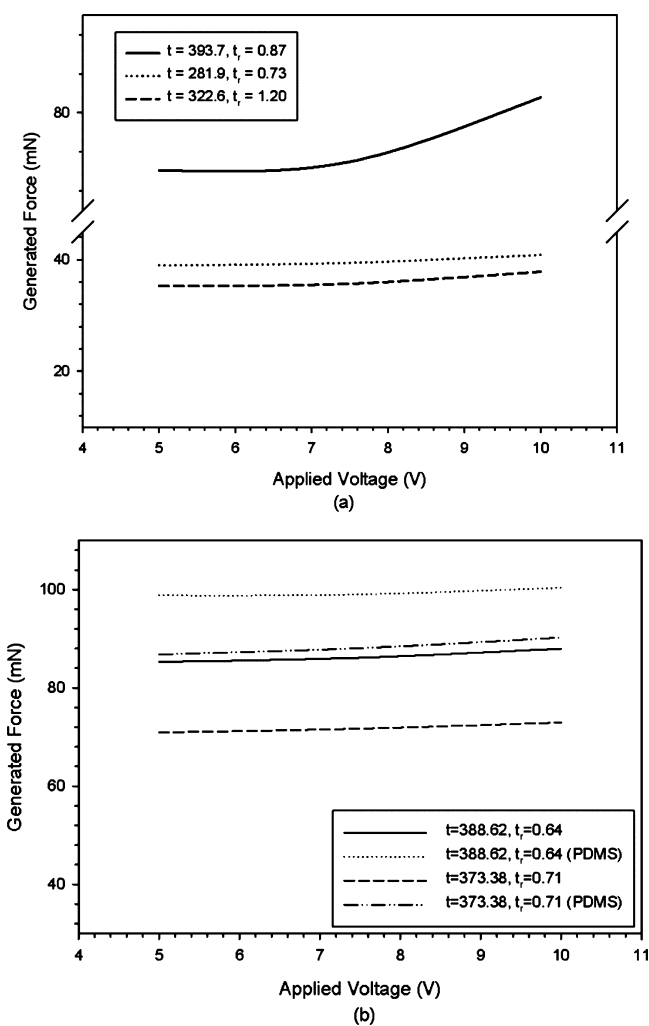


Figure 3. (a) Generated forces of BGA samples with different thicknesses (μm) and thickness ratios at different applied voltages; (b) generated force of two BGA samples before and after casting the PDMS layer.

thickness ratio also play an important role on BGA performance. It was reported that BGA displacement decreased linearly with increase in BGA total thickness.¹¹ In addition, BGA samples with thickness ratio between 0.9 and 2.5 showed improvement in their displacement.¹¹ In this study, BGA samples with higher thicknesses and lower thickness ratios (i.e., thinner electrolyte layers) displayed higher generated forces. BGA samples covered with the PDMS layer were also evaluated

to observe the effect of this layer on generated force. The generated force was increased by $\sim 14\text{--}23\%$ when PDMS layer was casted on the same samples (Figure 3). The range of calculated forces was compared to similar cases in the literature (Table 1), and consequently the generated force concern was resolved.

Bubble Generation (hydrolysis). The second concern addressed in the feasibility study was bubble generation (hydrolysis), which is a common issue in utilizing electroactive materials in microfluidics.²⁴ The BGA samples were operated underwater, and no visible bubble generation was observed for driving voltages of 2–10 V. In addition to a rapid response time, low driving voltage, and easy fabrication process, the lack of bubbles and sufficient generated force made BGA a promising candidate in microfluidic applications.

2.3. Flow Regulator. Design and Fabrication. A flow regulator was designed to study the efficiency of the BGA as a microvalve. This device consisted of two major parts: a base part and a transparent PMMA cover (Figure 4). Instead of a fixed channel with a certain shape and size, a tube-housing was considered in the design. Therefore, by using tubes with various inner diameters, we could study different cross-sectional areas. A secondary smaller chamber was utilized in the base part to isolate the electrical contacts from the passing fluid while BGA had to be in direct contact.

The base part of the flow regulator was fabricated using a 3D printing technique. V-Flash FTI 320 desktop modeler was employed for this process. The cover part was cut from a PMMA sheet with a thickness of 3 mm. The cover was then assembled on the printed base part using four M4 \times 10 bolts.

Flow Rate Measurement. An experimental apparatus was designed to carry out the flow rate measurements. Bartels MP6 micropump was utilized to provide a constant input for the flow regulator. Water was chosen as the fluid for all tests in this study. Tygon tubes were used for connecting the reservoir, micropump, flow regulator, and the output.

The micropump was driven by a SRS-shape signal at 100 V and 80 Hz. The BGA microvalve was driven by a rectangular signal at three different voltages (5, 8, 10 V) and six frequencies (250, 125, 100, 50, 25, and 10 mHz). Varying voltage and frequencies were applied to check their influence on flow regulation. In this study, applied voltage of 10 V was tested to evaluate the maximum blocking force of the BGA microvalve. However, for routine operation, applied voltage should be kept under 5 V. At voltages higher than 5 V, the ionic liquid starts to decompose, and hence, the BGA displacement and efficiency would decrease over time.¹¹ BGA was driven at 50% duty cycle (BGA valve was ON at half of the period and was OFF for the other half). Flow rate tests were also conducted at zero frequency (100% ON) to measure the leakage of the valve.

Flow rate was measured by weighing the output of the system over a certain sampling time. Sampling times were selected based on the frequency at which the BGA was being operated, and it was assured that the sampling time was a multiple of the time period. Each test was repeated three times to evaluate the repeatability of the data. The average flow rate and standard deviation of each test is presented in Figure 5.

3. RESULTS AND DISCUSSION

The output flow rate of the flow regulator as different applied voltages and frequencies was calculated and compared to input flow rate (OFF microvalve mode). The output flow rate was observed to be a function of both voltage and frequency. BGA

Table 1. Generated Force of Several Reported Microvalves and Their Typical Limitations

reference	type/material	valve size (mm)	applied power	force	limitations
Kwon ²⁴	hydrogel	4 × 0.3 × 0.1	15 V	7 mN	Slow response time, Bubble generation, No precise motion control
Tamanaha ²⁹	SMA wire and bead	∅1.12 × 1.47		2.35 N	Slow response time
Ren ²⁶	electromagnetic	4.5 × 0.1 × 0.1	1.25 A	5 mN	Complicated structure
Meckes ²⁷	electromagnetic	8 × 6 × 0.02	0.025 A	0.8 mN	
force measurements	BGA (<i>t</i> = 281.9 μm, <i>t_r</i> = 0.73)	30 × 8 × 0.28	10 V	41 mN	
	BGA (<i>t</i> = 322.6 μm, <i>t_r</i> = 1.20)	30 × 8 × 0.32	10 V	38 mN	
	BGA (<i>t</i> = 393.7 μm, <i>t_r</i> = 0.87)	30 × 8 × 0.39	10 V	80 mN	

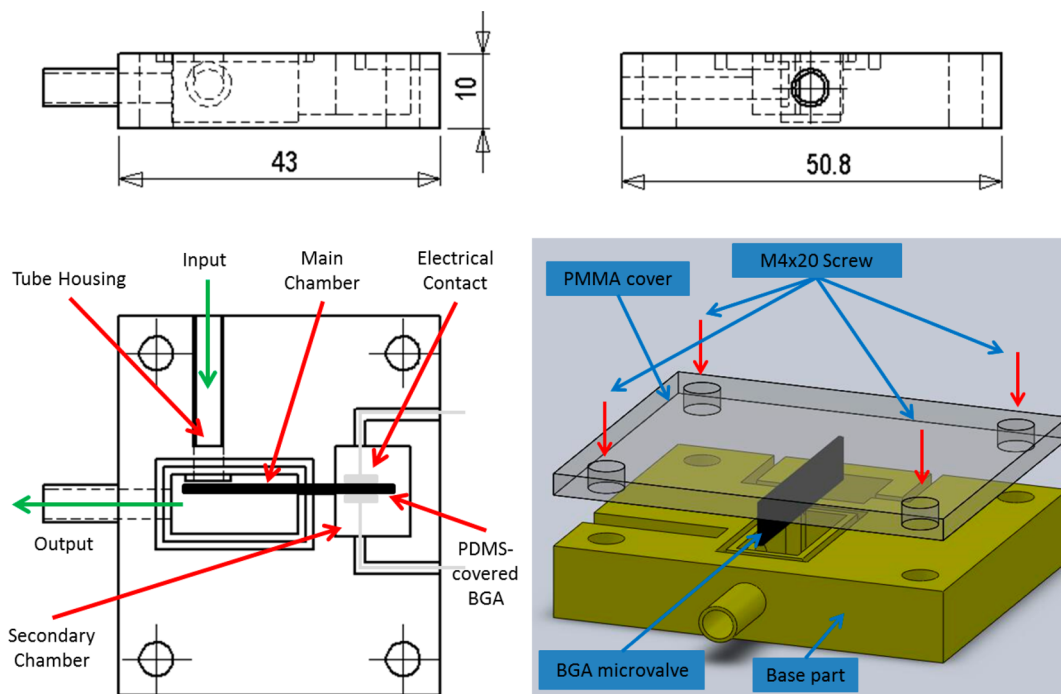


Figure 4. Schematics of the base part and the exploded view of the flow regulator assembly.

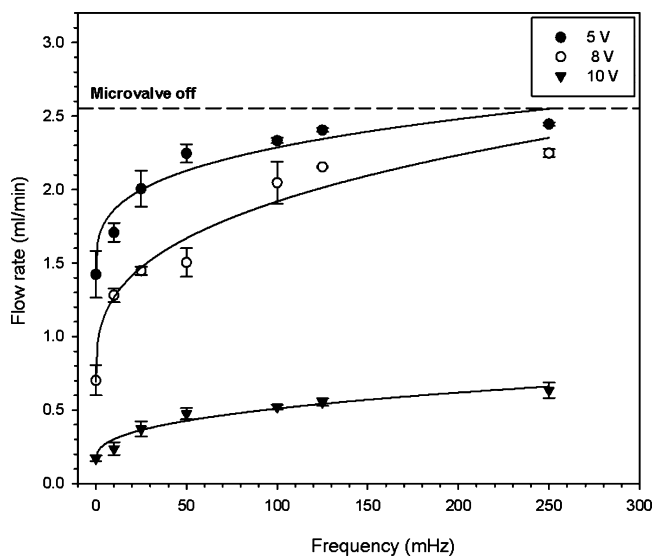


Figure 5. Measured flow rate at different frequencies and three different voltages. BGA was driven under a rectangular shape signal with 50% duty cycle.

microvalve performance was noticeably correlated with voltage. The average output flow rate at the voltage of 10 V was reduced almost four times (from 1.626 to 0.423 mL/min) compared to at 8 V. Similarly, applied frequency was influential on BGA microvalve performance. The output flow rate was reduced when frequency was, displaying a polynomial trend. The flow rate was lowered up to 45, 72, and 93% (compared to OFF microvalve) by reducing the frequency, while the voltage was kept constant at 5, 8, and 10 V, respectively (Figure 5). In case of higher applied voltages (8 and 10 V), the output flow rate was significantly reduced at the frequency of zero (100% ON mode), but did not reach zero (Figure 5). BGA microvalve showed leakage of 1.393, 0.702, and 0.171 mL/min at 8 and 10 V, respectively.

On the basis of these observations, it was concluded that different ranges of flow rate can be achieved for different applications by BGA microvalve. Output flow rate can be adjusted through varying different parameters such as applied voltage, frequency, driving signal shape, BGA thickness and thickness ratio, and channel/tube section area. Moreover, the order of output flow rate can be drastically reduced by altering the microvalve design. BGA diaphragm or miniaturized in-channel valve would be a successful step toward achieving lower flow rates (μL/min and nL/min). BGA microvalve would be

applicable in point-of-care devices for biomedical studies, diagnostics, drug delivery, DNA amplification, etc., when such low output flow rates are achieved. BGA microvalve performance also suggested that application of this material in microfluidics can be extended beyond just flow regulation. Micropumping and mixing with BGA appears to be within reach, if proper modifications in design are applied.

4. CONCLUSIONS

BGA was reported as new interface for flow regulation in microfluidics. BGA was utilized as a microvalve with low driving voltage, rapid response, simple fabrication process, and low power consumption, which is also easy to integrate. Feasibility studies were conducted to address two primary concerns of utilizing BGA microvalve: actuation force and bubble generation. Following the promising results, a flow regulator utilizing this BGA microvalve was designed and fabricated. Flow rate measurements were carried out and it was observed that output flow rate was reduced up to 93% based on the applied voltage and frequency. The BGA microvalve demonstrated the potential to be used for flow regulation in point-of-care devices for life science studies, drug delivery, and biomedical applications.

■ ASSOCIATED CONTENT

Supporting Information

Supporting Information has been provided on the following topics: BGA lifetime, effect of thickness and thickness ratio on BGA displacement, effect of PDMS layer on BGA generated force, and experimental apparatus for measuring the flow rate. This material is available free of charge via the Internet at <http://pubs.acs.org/>.

■ AUTHOR INFORMATION

Corresponding Author

*E-mail: ali.k.ghamsari@gmail.com. Phone: (225) 771-2700. Fax: (225) 771-4877.

Notes

The authors declare no competing financial interest.

■ ACKNOWLEDGMENTS

The authors express their gratitude toward National Science Foundation (Award 0932300) for supporting Next Generation Composite Crest Center (NextGenC³) in this study.

■ REFERENCES

- (1) Fukushima, T.; Asaka, K.; Kosaka, A.; Aida, T. *Angew. Chem., Int. Ed.* **2005**, *44* (16), 2410–2413.
- (2) Tunckol, M.; Durand, J.; Serp, P. *Carbon* **2012**, *50* (12), 4303–4334.
- (3) Yu, P.; Yan, J.; Zhao, H.; Su, L.; Zhang, J.; Mao, L. *J. Phys. Chem. C* **2008**, *112* (6), 2177–2182.
- (4) Mundaca, R. A.; Moreno-Guzmán, M.; Eguílaz, M.; Yáñez-Sedeño, P.; Pingarrón, J. M. *Talanta* **2012**, *99* (0), 697–702.
- (5) Liu, X.; Li, L.; Zhao, X.; Lu, X. *Colloids Surf., B* **2010**, *81* (1), 344–349.
- (6) Liu, T.; Zhu, X.; Cui, L.; Ju, P.; Qu, X.; Ai, S. *J. Electroanal. Chem.* **2011**, *651* (2), 216–221.
- (7) Liu, X.; Ding, Z.; He, Y.; Xue, Z.; Zhao, X.; Lu, X. *Colloids Surf., B* **2010**, *79* (1), 27–32.
- (8) Zhan, X.-M.; Liu, L.-H.; Gao, Z.-N. *J. Solid State Electrochem.* **2011**, *15* (6), 1185–1192.
- (9) Choi, B. G.; Park, H.; Park, T. J.; Kim, D. H.; Lee, S. Y.; Hong, W. H. *Electrochem. Commun.* **2009**, *11* (3), 672–675.

- (10) Ghamsari, A. K.; Jin, Y.; Woldesenbet, E. *Smart Mater. Struct.* **2012**, *21* (4), 045007.
- (11) Ghamsari, A. K.; Jin, Y.; Zegeye, E.; Woldesenbet, E. *Smart Mater. Struct.* **2013**, *22* (2), 025034.
- (12) Terasawa, N.; Takeuchi, I. *Sens. Actuators, B* **2010**, *145* (2), 775–780.
- (13) Bisio, M.; Ansaldo, A.; Futaba, D. N.; Hata, K.; Ricci, D. *Phys. Status Solidi B* **2010**, *247* (11–12), 3055–3058.
- (14) Bisio, M.; Ansaldo, A.; Ricci, D. *Phys. Status Solidi RRL* **2010**, *4* (3–4), 64–66.
- (15) Bisio, M.; Ansaldo, A.; Futaba, D. N.; Hata, K.; Ricci, D. *Carbon* **2011**, *49* (7), 2253–2257.
- (16) Bisio, M.; Ansaldo, A.; Picardo, E.; Ricci, D. *Carbon* **2012**, *50* (12), 4506–4511.
- (17) Bisio, M.; Ansaldo, A.; Ricci, D. *Phys. Status Solidi B* **2012**, *249* (12), 2361–2364.
- (18) Sugino, T.; Kiyohara, K.; Takeuchi, I.; Mukai, K.; Asaka, K. *Sens. Actuators, B* **2009**, *141* (1), 179–186.
- (19) Takeuchi, I.; Asaka, K.; Kiyohara, K.; Sugino, T.; Terasawa, N.; Mukai, K.; Shiraishi, S. *Carbon* **2009**, *47* (5), 1373–1380.
- (20) Torop, J.; Sugino, T.; Asaka, K.; Jänes, A.; Lust, E.; Aabloo, A. *Sens. Actuators, B* **2012**, *161* (1), 629–634.
- (21) Fukuda, K.; Sekitani, T.; Zschieschang, U.; Klauk, H.; Kuribara, K.; Yokota, T.; Sugino, T.; Asaka, K.; Ikeda, M.; Kuwabara, H.; Yamamoto, T.; Takimiya, K.; Fukushima, T.; Aida, T.; Takamiya, M.; Sakurai, T.; Someya, T. *Adv. Funct. Mater.* **2011**, *21* (21), 4019–4027.
- (22) Sugino, T.; Asaka, K. In *Proceedings of the 2011 SICE Annual Conference (SICE)*; Tokyo, Sept 13–18, 2011; The Society of Instrument and Control Engineers: Tokyo, 2011; pp 1696–1697.
- (23) Fang, Y.; Tan, X. *Sens. Actuators, A* **2010**, *158* (1), 121–131.
- (24) Kwon, G. H.; Choi, Y. Y.; Park, J. Y.; Woo, D. H.; Lee, K. B.; Kim, J. H.; Lee, S.-H. *Lab Chip* **2010**, *10* (12), 1604–1610.
- (25) Santos, J.; Lopes, B.; Branco, P. J. C. *Sens. Actuators, A* **2010**, *161* (1–2), 225–233.
- (26) Ren, H.; Gerhard, E. *Sens. Actuators, A* **1997**, *58* (3), 259–264.
- (27) Meckes, A.; Behrens, J.; Kayser, O.; Benecke, W.; Becker, T.; Müller, G. *Sens. Actuators, A* **1999**, *76* (1–3), 478–483.
- (28) Rosset, S.; Shea, H. *Appl. Phys. A: Mater. Sci. Process.* **2012**, *1*–27.
- (29) Tamanaha, C. R.; Whitman, L. J.; Colton, R. J. *J. Micromech. Microeng.* **2002**, *12* (2), N7.